Global Ecology and Conservation 24 (2020) e01299

Contents lists available at ScienceDirect

Global Ecology and Conservation

journal homepage: http://www.elsevier.com/locate/gecco

Original Research Article

Understanding global spatio-temporal trends and the relationship between vegetation greenness and climate factors by land cover during 1982–2014

Munkhnasan Lamchin [a, b], Sonam Wangyel Wang [a], Chul-Hee Lim [a], Altansukh Ochir [b], Ukrainskiy Pavel [c], Belay Manju Gebru [d], Yuyoung Choi [d], Seong Woo Jeon [d], Woo-Kyun Lee [d, *]

[a] Ojeong Eco-Resilience Institute (OJERI), Korea University, Korea University, 145, Anam-Ro, Seongbuk Gu, Seoul, 02841, Republic of Korea
[b] Department of Environment and Forest Engineering, School of Engineering and Applied Sciences, Institute for Sustainable Development, National University of Mongolia, Ulaanbaatar, 210646, Mongolia
[c] Centre for Aerospace and Ground Monitoring of Objects and Natural Resources, Belgorod National Research University, Belgorod, 308015, Russia
[d] Department of Environmental Science and Ecological Engineering, Korea University, Korea University, 145, Anam-Ro, Seongbuk Gu, Seoul, 02841, Republic of Korea

ARTICLE INFO

Article history:
Received 14 March 2020
Received in revised form 25 September 2020
Accepted 25 September 2020

Keywords:
Vegetation greenness trends
Precipitation
Temperature
Global
Land cover
Correlation

ABSTRACT

Analysis of the correlation between vegetation greenness and climate variable trends is important in the study of vegetation greenness. Our study used Normalized Difference Vegetation Index-3rd generation data from the Advanced Very High-Resolution Radiometer - Global Inventory Modeling and Mapping Studies (AVHRR-GIMMS NDVI3g), land cover data from the Climate Change Initiative (CCI-LC), and climate data from the Climatic Research Unit global time series (CRU TS) of climate variables (temperature and precipitation, solar radiation) over the past 33 years. First, we estimated the overall trends for vegetation greenness and climate variables over five time periods. Second, we subjected the data to correlation, regression, and residual analyses to detect correlations between vegetation greenness and different climate variables. Third, we extracted trends and correlation results by primary land cover types for each climate zone. Our study was focused at the global scale, and findings indicate that the largest decreasing trend of vegetation greenness and grasslands occurred in the mid-latitude regions of the Northern Hemisphere and in parts of South America, Africa, Saudi Arabia, and south and northeast Asia. In particular, the cold climatic zones of forest (36.6%), cropland (36.6%), and grassland (14.1%) suffered significant decline in vegetation greenness. Anthropogenic activities are mainly responsible for declining vegetation greenness particularly in northern Africa, central and western Asia. However, residual analysis shows an increase in vegetation greenness in some parts of western Europe, southern Australia, and the northern part of South America. The study also identified temperature and precipitation as the main factors responsible for controlling vegetation growth. Hot-spot areas with the largest temperature increases were found in the Amazon, Central America, southern Greenland, east Africa, south-east Asia, and other areas. However, temperatures decreased in the western part of South America, Angola, the Philippines, Indonesia, and Papua New Guinea. Precipitation decreased the

* Corresponding author. Tel.: +82-2-3290-3016.
E-mail addresses: nasaa@korea.ac.kr (M. Lamchin), wangsonam@korea.ac.kr (S.W. Wang), limpossible@korea.ac.kr (C.-H. Lim), altansukh@seas.num.edu.mn (A. Ochir), ukrainski@bsu.edu.ru (U. Pavel), bmanjur@korea.ac.kr (B.M. Gebru), cuteyu0@korea.ac.kr (Y. Choi), eepps_korea@korea.ac.kr (S.W. Jeon), leewk@korea.ac.kr (W.-K. Lee).

https://doi.org/10.1016/j.gecco.2020.e01299

most from March to May over most parts of the world with high correlation (r = 0.88) in Russia Canada, northeast Asia, and central Africa. In general, climate factors were the principal drivers of the variation in vegetation greenness globally in recent years.

1. Introduction

Understanding the dynamics of vegetation greenness and its correlation with climate variable is an important process in understanding current situations and project future changes (Tucker and Nicholson, 1999; Eklundh and Olsson, 2003; Luo et al., 2020). Such information is crucial for sustainable land use planning, developing resource use policies, and disaster preparedness (Jin et al., 2019). Vegetation greening is defined as a statistically significant increase in annual or seasonal vegetation greenness at a given location (Piao et al., 2019). Vegetation greening may be caused by many factors including temperature, precipitation, solar radiation, increases in average leaf size, leaf number per plant, plant density, species composition, duration of green-leaf presence due to changes in the growing season, and number of crops grown per year (Yu et al., 2016). In the past Rasmus Fensholt et al. (2012) used AVHRR to analyze global trends in vegetation greenness in Earth's arid and semi-arid lands. On the other hand, De Jong et al. (2012), Chen et al. (2019) and Yao et al. (2019) estimated vegetation greenness based on only NDVI. However, some studies have focused on the relation between NDVI and LAI that has showed high exponential relationships with LAI (Buermann et al., 2002).

Changes in vegetation greenness have been proven to increase the uncertainties of the projected changes of the annual means in surface fluxes and conditions, with stronger impacts on changes in sensible heat flux than on evapotranspiration (ET), soil water content, or surface runoff (Purdy et al., 2018). In particular, regions within approximately 50–70° N latitude in central and east Asia, northwestern north America, and the Amazon, exhibit high degree of uncertainties due to projected Leaf Area Index (LAI) changes. In addition, climate variables have been proven to affect vegetation greenness (Zeng et al., 2005; Fensholt et al., 2009; Fu et al., 2015). The Tibetan Plateau was identified as another region where large uncertainties are found for the projected changes in vegetation and climate (Yu et al., 2016).

Analysis of trends between the changes in vegetation greenness, temperature, precipitation, and solar radiation are important for designing interventions to mitigate the negative impacts of climate change, human activity, and natural disasters on the well-being of society and the environment. The Advanced Very High Resolution Radiometer (AVHRR) Global Inventory Modeling and Mapping Studies (GIMMS) Normalized Difference Vegetation Index (NDVI) 3 g data are popular tools for analyzing vegetation trends at the regional to global scale as evidenced in several past studies by Anyamba and Tucker (2005); de Jong et al. (2011); Eklundh and Olsson (2003); Helldén and Tottrup (2008); Jeyaseelan et al. (2007); Myneni et al. (1998); Olsson et al. (2005); Slayback et al. (2003); and Tucker et al. (2001). Same methods have also been applied to detect changes in vegetation phenology by Heumann et al. (2007); Myneni et al. (1997); and Stockli and Vidale (2004). Studies by Zeng et al. (2005), Fensholt et al. (2009), and Fu et al. (2015) have attempted to ascertain the causal factors responsible for the observed changes in vegetation greenness by investigating the response of vegetation vigor to climatic variations, represented by variables such as precipitation and air temperature. Researchers (Fensholt and Rasmussen, 2011; Tian et al., 2015; Zhao et al., 2018) have asserted that GIMMS NDVI3g data demonstrate good reliability for long-term trend analysis in arid regions, as long as provisions for humid, sub-humid, semi-arid, and hyper-arid regions due to temporal discordances between sensors are present. To address such uncertainties in the satellite-observed trends in vegetation growth, Guo et al. (2018) recommended more comprehensive analysis to compute an NDVI time series against field measurements and multi-scale imagery, before attempting trend analysis to acquire demonstrative results (Guay et al., 2014).

A recent study by Yu et al. (2016) indicated a decreasing precipitation trend in the regions of the Mediterranean, southwestern North America, most of south America, and South Africa, accompanied by an increasing trend in the areas of the Northern Hemisphere, south Asia, and the maritime subcontinent. A study by Jeyaseelan et al. (2007) reported that the global mean surface temperature has increased by 0.85 °C during the period 1880–2012 and that this increase is accompanied by an increase of 0.12 [0.08–0.14] °C per decade^{-} in global land and ocean temperatures over the past 60 years (Jeyaseelan et al., 2007). However, the amount of warming during the last 15 years (0.05 °C/decade^{-1}) is significantly lower than the number computed since 1951 (Jeyaseelan et al., 2007). During this warming hiatus (Kosaka and Xie, 2013), observational data exhibited a continued increase in hot extremes over land (Seneviratne et al., 2014). Biological events in plant phenology are powerful indicators of the seasonality of the environment, expressing the implicit meaning of rising temperatures on the vegetation function (Cleland et al., 2007; Zeng et al., 2011; Stockli and Vidale, 2004; Peñuelas et al., 2009). Past research (Trenberth et al., 2014) has indicated that an increase in temperature from global climate change could intensify droughts. In addition, some studies (Whittaker, 1975; Churkina and Running, 1998) have also shown that plant growth in the northern latitudes is limited by the temperature and length of the growing season. It has also been shown that springtime warming in the northern Hemisphere is associated with the observed increases in photosynthetic activity, or vegetation "greening" trends (Myneni et al., 1997; Tucker et al., 2001; Zhou, 2001; Nemani et al., 2003; Wang et al., 2011; Xu et al., 2013). Wolkovich et al. (2012) estimated the growing season onset in the northern Hemisphere to be

1.1–3.3 days per decade. Past studies have generated useful information for planning land management at regional scales. However, there is a need to use long term data to better understand vegetation greenness trends at global levels and its interactions with climate and human factors. To respond to this need, we used Advanced Very High Resolution Radiometer (AVHRR) Global Inventory Modeling and Mapping Studies (GIMMS) Normalized Difference Vegetation Index (NDVI) 3 g to study global Spatio-temporal trends and the relationship between vegetation greenness and climate factors by land Cover types. The main differences between the results of this study and pervious study primarily showed trend of frequencies by each ten years for NDVI, temperature and rainfall, solar radiation, and relation between of vegetation greenness and climate factors by land cover type in climate zone.

In particular, our study provides: i) an analysis of the overall and seasonal trends of vegetation greenness and climate variables; and ii) correlations and multi-linear regression between vegetation greenness and precipitation and temperature, extracted by primary land cover type. Whereas the majority of past studies has largely focused on the long-term assessment of vegetation greenness, our study attempts to ascertain decadal changes in the overall trends in vegetation greenness and climate variables by primary land cover type in each climate zone at a global scale. Specifically, our study aims to answer the following questions: (i) What are the dynamic trends of global vegetation greenness, precipitation, and temperature during the period 1982–2014 and how have they changed in each decade? (ii) What is the seasonality (four-season) trends of global vegetation greenness, precipitation, and temperature during the same time period? (iii) Which results show correlations between vegetation greenness and climatic factors and climate control on vegetation greenness? (iv) What is the vegetation greenness, the climate causal factors for the trend and correlation observed by primary land cover type (forest, cropland, and grassland) and the trend of vegetation greenness by primary land cover type in each climate zone? These findings will not only contribute to the analysis of vegetation greenness but also have great significance in predicting the effects of climate change on global vegetation greenness and primary land cover types.

2. Materials and methods

2.1. Data acquisition

2.1.1. Remote sensing vegetation data

The GIMMS-NDVI3g dataset derived from US National Oceanic and Atmospheric Administration's (NOAA's) AVHRR satellite record is the most recent version of the NDVI (Fensholt et al., 2012). Compared to the datasets from other sources, such as the U.S. National Aeronautics and Space Administration's (NASA's) Moderate Resolution Imaging Spectroradiometer (MODIS, February 2000–present), the GIMMS-NDVI3g dataset is the longest global sub-monthly time series of the greenness index. NDVI3g data were collected to represent the 33-year period spanning from 1982 to 2014 with a spatial resolution of 8 km and calculated using the average monthly NDVI from January to December (https://ecocast.arc.nasa.gov/data/pub/gimms/). Also, we used GIMMS-LAI3g version 2.

2.1.2. Climate data

Data on the monthly average daily maximum temperature (°C) and precipitation (mm per month) were collected from the Climatic Research Unit Time Series (CRU TS), University of East Anglia (CRU TS v. 4.01, https://www.cru.uea.ac.uk/, Harris et al. (2014)). The dataset has a resolution of $0.5^\circ \times 0.5^\circ$ and is based on the analysis of records from over 4000 individual weather station records. While the dataset makes up a large proportion of the total input records, the dataset has been homogenized and Monthly shortwave radiation (SWD) data with a resolution of 0.5° was obtained from the CRU National Centers for Environmental Prediction (CRU-NCEP) v7 data set. We used the monthly climate data of the same period as the NDVI time series (1982–2014), with the average monthly temperature and precipitation of the entire season from January to December and a total of 1188 data records for 396 months, in which one image is composed of 9,331,200 pixels.

2.1.3. Land cover data

The CCI 300 m annual global land cover time series from 1992 to 2015 was released by the Climate Change Initiative (CCI) land cover partnership https://www.esa-landcover-cci.org/(Feng et al., 2015). Five different satellite missions support the reprocessing of the land-cover data. The ENVISAT-MERIS full and reduced resolution reflectance dataset recorded from 2003 to 2012 is the main data source for land-cover discrimination, owing to its 15 spectral bands at 300 m resolution. The CCI data comprise the NOAA-AVHRR HRPT (high-resolution picture transmission) dataset, recorded at 1 km covering the period from 1992 to 1999. The AVHRR dataset, along with the SPOT-Vegetation time series spanning from 1998 to 2012 and the PROBA-V from 2013 to 2015 are used for land-cover detection. Using these datasets, annual global land-cover maps are produced at a 1 km resolution to serve as input to the change detection algorithm.

2.2. Methodology

2.2.1. Preprocessing

As CRU-TS and GIMMS-NDVI3g data were provided as NetCDF format from the original source, we converted the NetCDF data to single-raster format. The output is a TerrSet format raster layer (Kvamme, 2018). Following the NDVI3g data (8 km), the data cell size was changed to 0.083 and is indicated in column 4320, row 2160. We then resampled from the original resolution of 0.5 ° × 0.5 ° for all climate data to an 8 km resolution by the downscale scenario model within the Climate Change Adaptation Modeler, which is used to produce a high-resolution image from a low-resolution image (Fig. 1)

The model works either by generating anomalies between the coarse-resolution future and baseline scenarios or using previously calculated anomalies at the coarse resolution, which are then applied to a fine-resolution baseline image to determine the fine-resolution future scenario. This model can be used for a single image or for multiple images contained in the climatology data. The downscaling method used here is one of the downscaling methods from Terrset software used for rescaling data to a higher resolution. A common use of these data is species scenario modeling, and the method described here is adapted from Tabor and Williams (2010).

2.2.2. Mann-Kendall monotonic trend

2.2.2.1. Temporal trend analysis. The Mann-Kendall monotonic trend is a non-parametric test used to determine trends in time-series data. The test considers the significance of the Theil-Sen (TS) slope (Sen, 1968). The advantage of this method is that the data does not require a normal distribution, and it is not sensitive to outliers in the dataset (Sen, 1968; Fensholt et al., 2012). The datasets are required to transform one rank order into another to demonstrate the steadily increasing and decreasing trends. Trends vary from −1 to +1. The +1 value represents a continuously increasing trend and −1 indicates a continuously decreasing trend (Neeti and Eastman, 2011). Pixels with significant trends in vegetation greenness were determined by Z scores of the non-parametric Mann-Kendall significance test at the 95% significance level, which is commonly recommended for trend test for the TS procedure (Eastman et al., 2009; Luo et al., 2019; Lyu et al., 2019). For each pixel, we examined trends for vegetation greenness and climate variables by using a non-parametric trend test technique (Mann–Kendall test) to evaluate trends for each month, for four seasons, and for each decade during the 33-year study period, considering the integrated vegetation greenness, temperature, and rainfall derived from the satellite NDVI product and CRU data. The Mann–Kendall statistic (S) is as follows:

$$S = \sum_{i=1}^{n-1} \sum_{j=i+1}^{n} sign(NDVI_j - NDVI_i)$$

In this equation, if $NDVI_j$ and $NDVI_i$ are the NDVI value of times i and j, then:

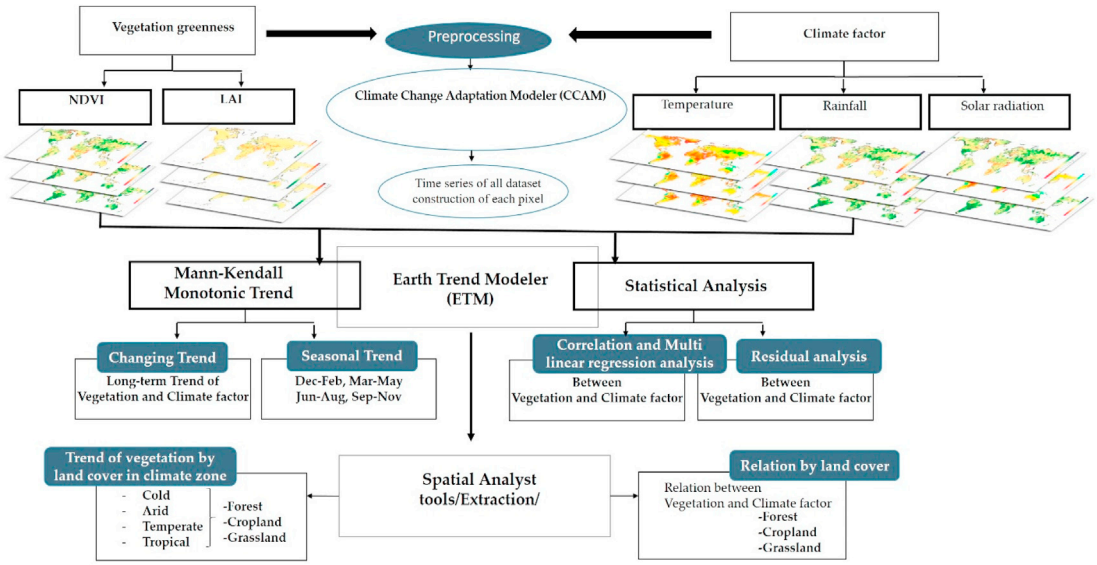

Fig. 1. Framework of the study.

$$sign(NDVI_j - NDVI_i) = \begin{cases} 1, \ if\,(NDVI_j - NDVI_i) > 0 \\ 0, \ if\,(NDVI_j - NDVI_i) = 0 \\ -1, \ if\,(NDVI_j - NDVI_i) < 0 \end{cases}$$

The variance of S is calculated as:

$$VAR(S) = \frac{n(n-1)(2n+5)}{18}$$

with n from 1982 to 2014 ($n = 33$).

The normalized test statistic Z is estimated as follows:

$$Z = \begin{cases} \dfrac{S-1}{\sqrt{VAR(S)}}, \ if\ S > 0 \\ 0, \ if\ S = 0 \\ \dfrac{S+1}{\sqrt{VAR(S)}}, \ if\ S < 0 \end{cases}$$

The statistic S is closely related to Kendall's t as given by:

$$t = \frac{S}{D}$$

$$\text{where.} D = \left(\tfrac{1}{2}n(n-1) - \tfrac{1}{2}\textstyle\sum_{j=1}^{p} t_j(t_j-1)\right)^{1/2} \left(\tfrac{1}{2}n(n-1)\right)^{1/2}$$

2.2.2.2. Seasonal trend analysis. The Mann-Kendall statistic for the *gth* season is calculated as:

$$Sg = \sum_{i=1}^{n-1} \sum_{j=i+1}^{n} sign(NDVI_{jg} - NDVI_{ig}), \ g = 1, 2, \ldots..m$$

According to Hirsch et al. (1982), the seasonal Mann-Kendall statistic, S1, for the entire series is calculated according to:

$$s = \sum_{g=1}^{m} s_g$$

2.2.3. Statistical analysis

We applied linear regression analysis to analyze the spatial and temporal fluctuations of the vegetation greenness and climate variables by assessing the per-pixel values from 33 years of overlay monthly observations (January 1982 to December 2014). Furthermore, we used correlation and multiple regression between vegetation greenness and climate factors such as rainfall and temperature at the global level. The correlation coefficient, denoted by r, is a measure of the strength of the linear relationship between two variables. Multiple regression describes how the changes in each independent variable are related to changes in the dependent variable. Regression also statistically controls every variable and estimates the effect that changing one independent variable has on the dependent variable while holding all the other independent variables constant.

Residual maps were created to identify the local differences more clearly. With the dependent variable of NDVI and the independent variables of temperature and precipitation for each pixel, we examined trends for vegetation greenness and the linear regression of each climate variable, using the multiple linear regression model. Residual analysis can segregate the NDVI changes caused by human activity from those resulting from climatic variations (Evans and Geerken, 2004). As described by Wessels et al (2012), the NDVI residuals were calculated for each pixel. The best relationship between the mean NDVI and climatic factors was acquired by using multiple correlation regression. Then, the predicted NDVI could be computed using this relationship. The NDVI residuals were obtained as the differences between the predicted and observed NDVI values. The residuals were also analyzed to detect trends over time. When the changing trend of the NDVI residuals was insignificant, changes in NDVI were explained by climatic trends. In contrast, when the changing trend of the NDVI residuals was significant, changes in the NDVI were not explained by climatic trends and may have been caused by human activity. Based on the linear regression method, the influences of human-induced vegetation changes were obtained. If the residuals show no trend over time, the observed changes in vegetation are considered to be affected by climatic factors. Meanwhile, a decreasing trend

indicates that human activity has a negative impact on vegetation cover changes and an increasing trend describes that human activities (afforestation and population migration are assumed) have contributed to vegetation growth.

We evaluated the statistical significance for 10 observations at different effect sizes. The calculation used the approach described by Cohen (1988) and was implemented in packages pwr and asbio for the R language. This approach links the type I error, type II error, sample size, and effect size. The minimum effect value is indicated, which is statistically significant for 10 years of observation. For a detailed clarification of the calculation mechanism, the authors can readily provide a script in R.

The technical background for the trend of vegetation greenness by primary land cover type in each climate zone and correlation by land-cover analysis was provided by ArcGIS 10.6. In this case, we used the Spatial Analyst tools/Extraction/ Extract by Mask tool we made mask for our image, such that each zone would be represented by pixels in the raster. This provides a raster, which is used to create a polygon of the area.

3. Results

3.1. Trend of vegetation cover change and climate factors in the five periods

At a global scale, our analysis at 10-year intervals shows that between 1982 and 2014, the overall vegetation greenness has decreased, with the largest decrease recorded in Argentina, western-south America, North America, Canada, Central Africa, North Africa, Saudi Arabia, South Asia, and northeast Asia. However, we found increased vegetation greenness in southern Australia, a small area in north Africa, the Amazon, the Sahel region of central Africa, Spain, India, and southeast China Fig. 2.2(e). For three 10-year time periods of this study, in most of the regions, vegetation greenness exhibited an upward trend (0.28−0.51) from 1993 to 2002. However, in the next ten-year period (2002−2014), most vegetation greenness decreased (−0.11 to −0.49) in the arid and semiarid regions and in the desert or sandy land, with smaller decreases in southern Africa, western Australia, South and North America, Canada, and Russia Fig. 2.2(b). We also estimated the precipitation trend for 3 time periods of 10 years each. It should be noted that the precipitation decreased in most areas over the past

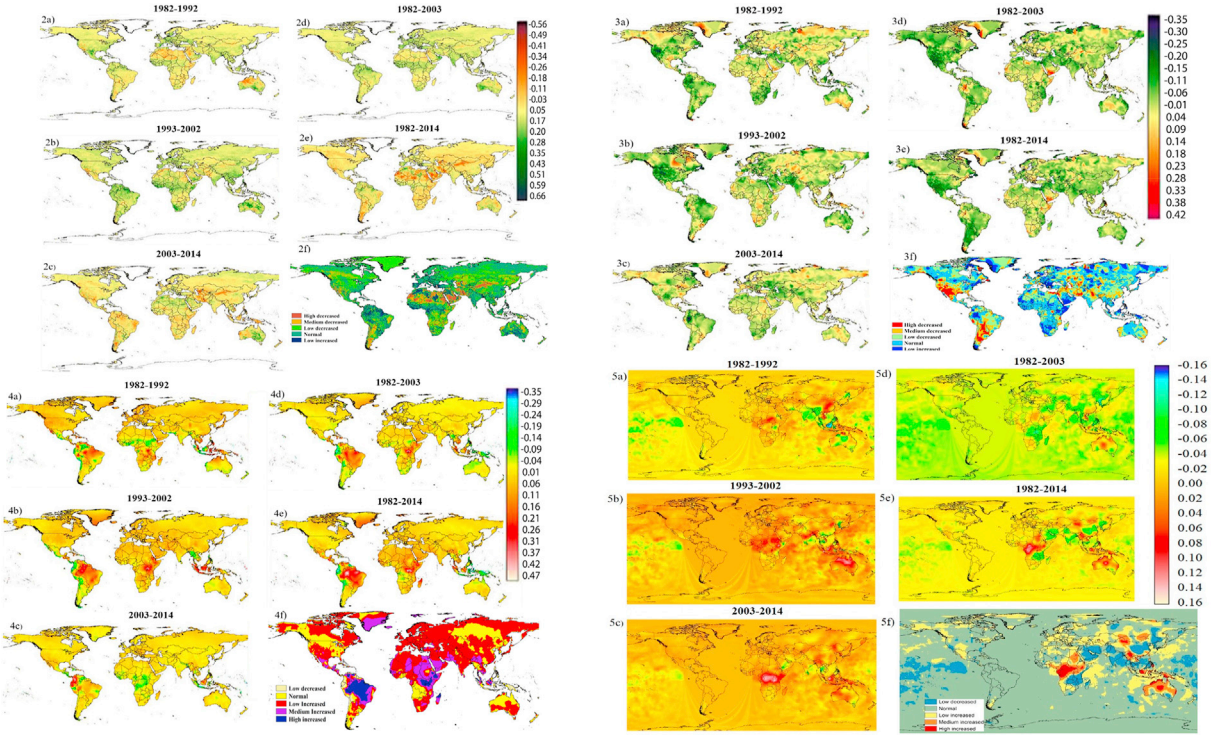

Fig. 2. 2.2. Overall trend of vegetation greenness for five periods 2a) 1982−1992; 2 b) 1993−2002; 2c) 2003−2014; 2 d) 1982−2003; 2e) 1982−2014. The index ranges from −0.56 to +0.66, and plus values denote a continuously increasing trend whereas minus values indicate a decreasing trend. 2f) Map of classified overall trend of vegetation greenness. 2.3. Overall trend of precipitation for five periods 3a) 1982−1992; 3 b) 1993−2002; 3c) 2003−2014; 3 d) 1982−2003; 3e) 1982−2014. The index ranges from −0.35 to +0.42, and plus values denote a continuously increasing trend whereas minus values indicate a decreasing trend. 3f) Map of classified overall trend of precipitation. 2.4. Overall trend of temperature for five periods 4a) 1982−1992; 4 b) 1993−2002; 4c) 20,032,014; 4 d) 1982−2003; 4e) 1982−2014. The index ranges from −0.35 to +0.47, and plus values denote a continuously increasing trend whereas minus values indicate a decreasing trend. 4f) Map of classified overall trend of temperature.2.5. Overall trend of solar radiation for five periods 5a) 1982−1992; 5 b) 1993−2002; 5c) 2003−2014; 5 d) 1982−2003; 5e) 1982−2014. The index ranges from −0.16 to +0.16, and plus values denote a continuously increasing trend whereas minus values indicate a decreasing trend. 5f) Map of classified overall trend of solar radiation.

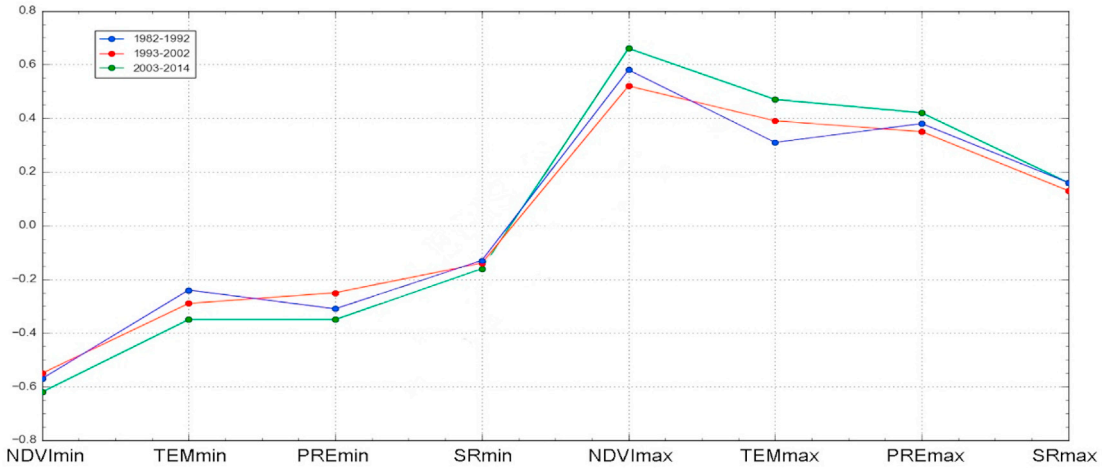

Fig. 3. Trend of NDVI min, max, Temperature min, max, Precipitation min, max and Solar radiation min max by 3 decades.

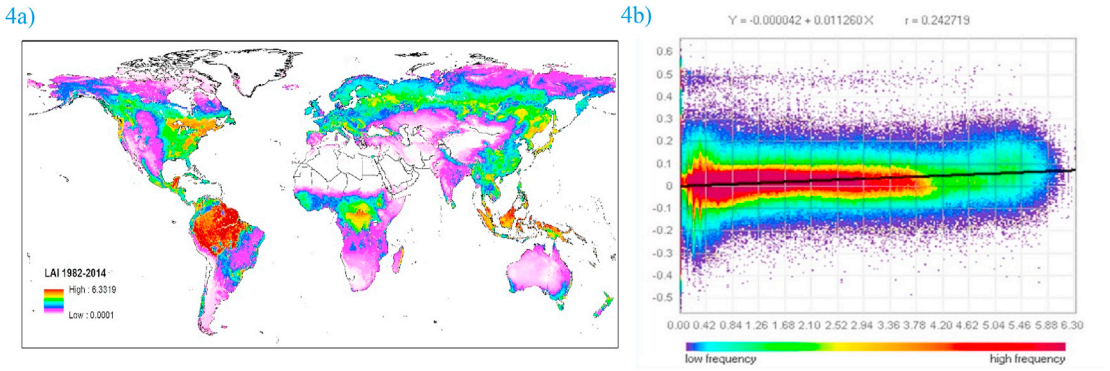

Fig. 4. Long term trend of Leaf area index (LAI) and correlation between NDVI and LAI.
4a) Trend of LAI 1982−2014, 4 b) Correlation between NDVI and LAI 1982−2014.

33 years Fig. 2.3(e). Nevertheless, in some smaller regions, an upward trend was observed, such as in Yemen in the Arabian Peninsula and in Somalia and Namibia in Africa. Results also indicate that during the last 33 years, the temperature increased the most in the Amazon, Central America, southern Greenland, east Africa, and Southeast Asia Fig. 2.4(e). However, western south America, Angola, the Philippines, Indonesia, and Papua New Guinea saw decreased temperatures. Those areas included in the equatorial zone showed the greatest upward and downward trend differences. From 1982 to 1992, most upward trends cover the central part of south America, south Africa, northern Australia, and south Asia, whereas most downward trends are located in the Sahel of Africa, some areas in south Asia, and northern South America.

The 1992−2002 period shows the same results as the previous decade in many areas except the Sahel of Africa, where the downward trend became an upward trend. The last cycle (2002−2014) shows a decreasing trend in the Sahel and other

Table 1
Results of seasonal trend analyses using Mann-Kendall test on the total grid points of last 33 year's climate variables data (Z).

Grid variable (1982−2014)	Trend	*P*	33 year	Winter	Spring	Summer	Autumn
Vegetation greenness	Positive (increasing)	0.05	1,866,240	3,265,920	1,399,680	3,172,608	2,799,360
	Negative (decreasing)	<0.01	4,665,600	3,545,856	2,985,984	5,878,656	3,639,168
Rainfall	Positive (increasing)	0.05	1,399,680	2,052,864	746,496	1,679,616	839,808
	Negative (decreasing)	<0.01	5,598,720	5,692,032	6,625,152	3,359,232	2,892,672
Temperature	Positive (increasing)	0.05	3,732,480	4,852,224	7,278,336	7,464,960	2,146,176
	Negative (decreasing)	<0.01	933,120	2,706,048	1,492,992	1,119,744	4,758,912
Solar radiation	Positive (increasing)	0.05	3,172,608	3,919,104	6,345,216	3,825,792	2,052,864
	Negative (decreasing)	<0.01	3,732,480	2,892,672	1,772,928	3,452,544	3,919,104

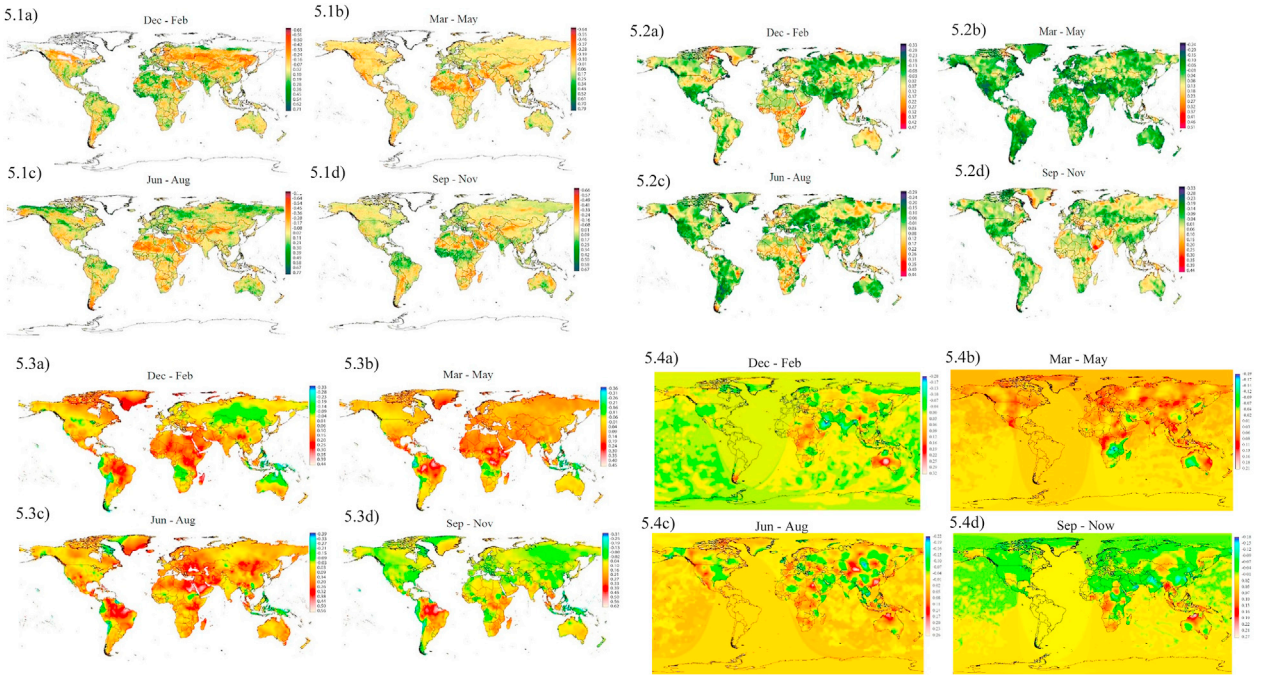

Fig. 5. Seasonal trend. 5.1) Seasonal trends of vegetation greenness, 5.2) Seasonal trend of precipitation, 5.3) Seasonal trend of temperature, 5.4) Seasonal trend of solar radiation over the last 33 years for the four seasons (plus value denotes a continuously increasing trend whereas the minus value indicates a decreasing trend.).

countries of central Africa, eastern south America, and some areas of south Asia and an increasing trend in northern south America. Generally, in the low latitudes (equatorial zone), the temperature increased from 1982 to 2003, but decreased from 2004 to 2014. Our analysis shows an overall decreasing solar radiation trend over the past 33 years in the mid-latitude region Fig. 2.5(e). However, solar radiation increased the most (0.04–0.12) in central Africa, northern Australia and central Asia regions. The graph of NDVI trend, Temperature, Precipitation, and Solar radiation by 3 decades showed in Fig. 3. Also, we explored the trend of Leaf area index (LAI) 1982–2014 and correlation between NDVI and LAI 1982–2014 (Fig. 4). NDVI showed medium exponential correlation with LAI and for graminoids was medium with R = 0.24.

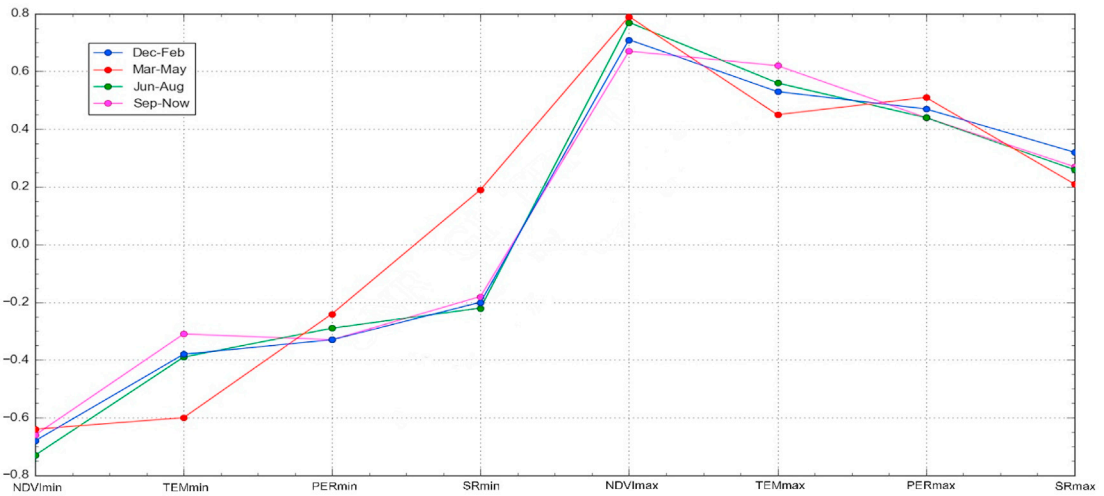

Fig. 6. Trend of NDVI min, max, Temperature min, max and Precipitation min, max, Solar radiation min, max by 4 seasons for 1982–2014.

Table 2
Trend of vegetation greenness by primary land cover type in each climate zone for 1982–2014 (area km^2 and %).

Primary cover type	Vegetation Greenness Trend	Climate zones							
		Cold km^2, %		Arid km^2%		Temperate km^2	%	Tropical km^2	%
Forest	Decreasing	4,788,771.22	26.8	–	–	–	–	3,546,754.38	23.5
	Normal	12,359,889.90	69.2	–	–	–	–	6,787,588.39	45.0
	Increasing	687446.60	3.8	–	–	–	–	4,730,514.79	31.4
Cropland	Decreasing	1,846,814.43	36.6	–	–	1,062,145.63	26.9	902706.87	24.4
	Normal	3,039,070.80	60.3	–	–	2,291,018.07	58.1	2,025,880.24	54.8
	Increasing	153,810.99	3.05	–	–	589,035.41	14.9	762,509.16	20.6
Grassland	Decreasing	418,302.22	11.9	1,478,899.45	25.7	299,919.48	14.1	–	–
	Normal	3,004,889.27	86.0	3,711,150.14	64.5	1,555,448.64	73.5	–	–
	Increasing	67,110.39	1.92	562,866.98	9.7	260,072.65	12.2	–	–

3.2. Seasonal trend analysis of vegetation greenness and climate variables

Findings of the overall seasonal trend analysis using Mann-Kendall test is presented in Table 1 and Figs. 5 and 6. It is show both increasing and decreasing trends at 0.05 and 0.01 significant levels for vegetation greenness, precipitation, temperature, and solar radiation across all the seasons. This is also evident from Fig. 5.1. In the first season (December to February), the largest amount of browning occurs in northeast Asia, central Asia, some regions of north America, southern Africa, and southern South America. However, a greening trend is detected in India, some areas of south Asia, the Sahel, north Africa, northern South America, central North America, and western Europe. The second season (March to May) shows a decreasing trend in the majority of areas. For the period from June to August, the results show the largest upward trend in northern Russia, Europe, northern North America, northern South America, and southern Australia. However, the largest decreasing trend occurs in northern and southern Africa and central Asia. The last analysis period is September to November, which shows an increasing trend in the Sahel, south Asia, Europe, and the Amazon, and the same decreasing trend as the previous period.

Seasonal precipitation trends are shown in Fig. 5.2. The largest decreasing trend ranged between −0.01 and −0.10 and occurred during the March–May season in most of the areas, with Kazakhstan (0.32) and western Russia (0.37) showing an increasing trend. June–August is the growing and summer season in the mid-latitude regions of the Northern Hemisphere; however, most of these regions show a decreasing trend for precipitation during all four seasons (−0.01 to − 0.10).

Seasonal temperature trends (Fig. 5.3) show decreasing temperatures (−0.02 to −0.19) across all of the Northern Hemisphere from September to November. Northeast Asia, north-central Asia, Russia, and northern Australia show a decreasing trend between December and February, whereas, over the four seasons, a decreasing trend is always observed in west-central Africa, the Philippines, Indonesia, Papua New Guinea, Peru, and Chile. In the other regions, increasing temperatures are

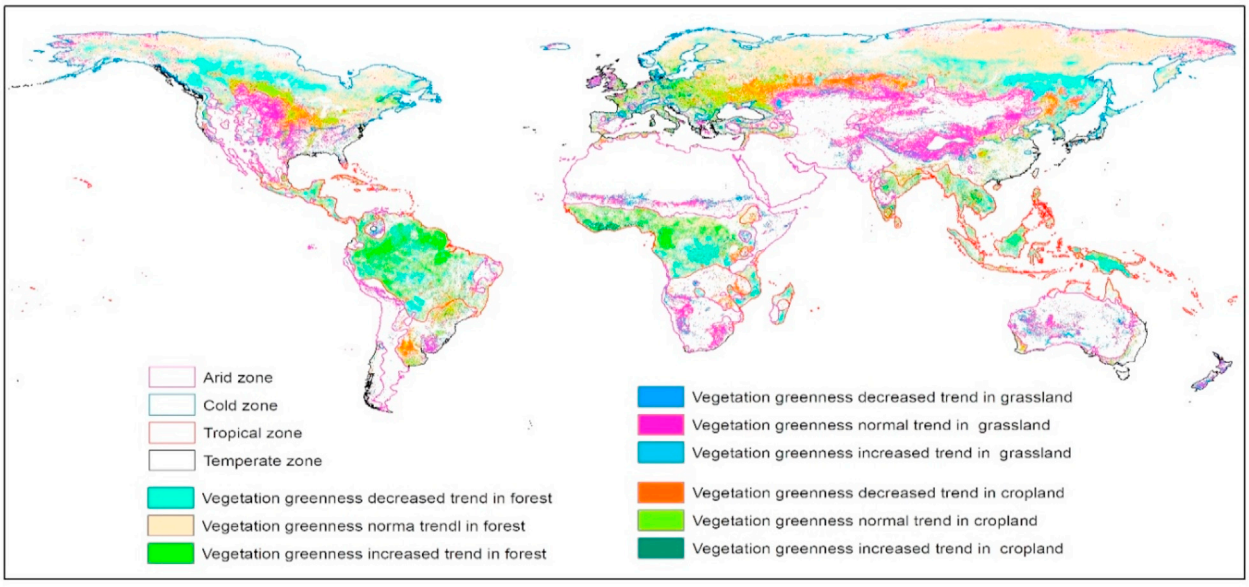

Fig. 7. The increasing and decreasing trend of vegetation greenness by primary land cover type for each climate zone.

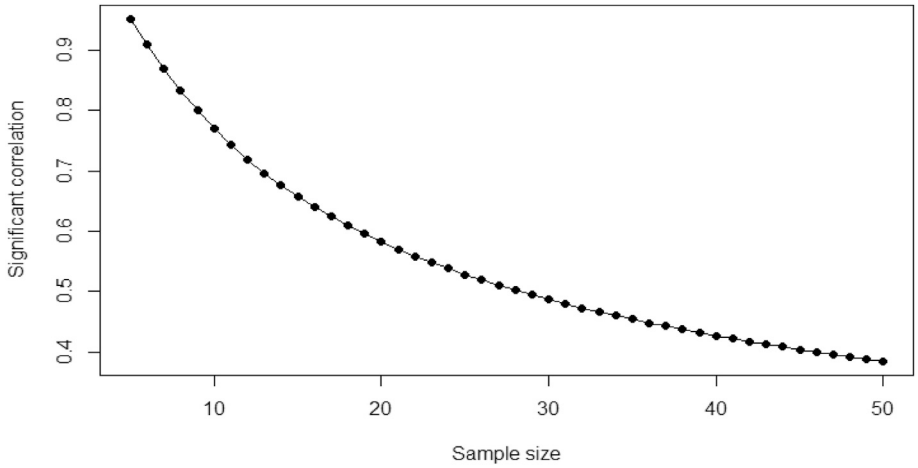

Fig. 8. Minimum statistically significant value of the correlation coefficient.

observed for all four seasons. Results also indicate that the temperature of the hot spot areas increased the most in the Amazon, southern Greenland, Madagascar, Ethiopia, Somalia, Kenya, Indonesia, Singapore, Malaysia, Cambodia, and southern Vietnam. In the spring, the Northern Hemisphere shows the largest temperature trend increase (0.14−0.35). Fu et al. (2015) reported that winter and spring temperatures have increased over the past three decades.

Fig. 5.4 shows the spatial distribution of the four season's solar radiation from 1982 to 2014. We observed relatively high increasing rate (0.06−0.16) of solar radiation in the north part of globally and spring season of march to May (Fig. 2 (5d)), however, were found decreasing rate (−0.07 to 0.17) in the southern Africa and western Australia.

3.3. Trend of vegetation greenness by land cover in climate zone

Compared with other climate zones in the forest, cropland, and grassland cover, the cold climate zone shows a fast decreasing vegetation greenness (Fig. 7). Our analysis also indicates higher increasing vegetation greenness in the forest and cropland areas in the tropical zone.

The study detected the largest decreasing trend of vegetation greenness in the forest cover of northeast Asia, southeast Russia, the part of Canada in the cold climate zone, and central Africa (Fig. 7). Because this trend occurred in the main forest land cover of the world, it may have an important impact on CO_2, which plays a major role in the global carbon balance. We examined the increased cropland area and confirmed the change in the trend of vegetation greenness for the cropland-covered areas. Most of the decreased vegetation greenness in the cropland was found in northeast China, North Korea, northern Kazakhstan, southwestern Russia, and eastern and southern Africa. However, in the cropland regions, the NDVI increased in north and east China, India, Europe, and North America. Our results are in agreement with the conclusion that cropland areas tend to increase in all regions (Huang et al., 2018) and that the increase in the peak vegetation growth occurred in areas of intense agricultural activities, such as northern China, India and North America. In cropland regions, the NDVI increased in central North America, India, and mid-eastern China (Guo et al., 2018). The trend of vegetation greenness for the grassland cover over the past 33 years has decreased in central, south, and northeast Asia, Australia, and Africa (Fig. 7).

In Table 2, we evaluated the area of the increasing and decreasing trend of the vegetation greenness by primary land cover type for each climate zone. The result suggests that 26.8% of the total forest cover of the cold zone exhibits decreasing vegetation greenness. Increasing vegetation greenness was observed in 31.4%, while a decreasing trend characterized 23.5% of the forest cover of the tropical zone. The cropland cold zone exhibits decreasing vegetation greenness by 36.6%. In the temperate zone, 26.9% of the total cropland showed decreasing vegetation greenness, and 20.6% showed an increasing trend. Generally, 11.9% of the cold zone exhibited decreasing vegetation greenness, and this decreasing trend was observed in 25.7% of the arid zone. However, only 14.1% of the grassland cover in the tropical zone demonstrated decreasing vegetation greenness during the last 33 years. In the cold climate zone, the forest, cropland, and grassland areas primarily exhibited decreasing vegetation greenness, indicating that more attention may need to be paid to the cold climate zone.

3.4. Regression analysis, correlations between vegetation greenness and climate factors by mainland cover

We computed the correlation coefficient, results of the analysis of test power (the analysis was made using the R language with the use of an additional package asbio) for the duration of the study at 10-year intervals. Overall, correlation coefficient values (r) larger than 0.77 are considered statistically significant (at 95% confidence level) however, correlation coefficients

larger than 0.58 and 0.47 are also considered statistically significant for 20 and 33 years, respectively (Fig. 8). The x axis indicates the duration of the study by decades and the Y axis shows NDVI values.

In this section, we estimated the extent to which vegetation greenness is controlled by climate variables (precipitation and temperature). Fig. 9 illustrates the climate control on vegetation greenness for the entire globe. Fig. 9(a) indicates a higher positive correlation value ($r = 0.64$) over most regions, confirming that precipitation is an important factor in the vegetation growth in the Northern Hemisphere, the southern part of Africa, and some parts of South America. However, negative correlation values were found in north Africa, the Amazon, southern South America, western North America some regions of south and southeastern Asia, western Australia, western Europe, a small area of India, and Myanmar. Meanwhile, the other cropland areas showed high correlation ($r = 0.87$). Vegetation greenness is controlled by temperature, showing a negative correlation between vegetation greenness and temperature $r = -0.53$ in most of the Northern Hemisphere, whereas a positive correlation was found in the Southern Hemisphere for cropland. We infer that while, temperature has the greatest

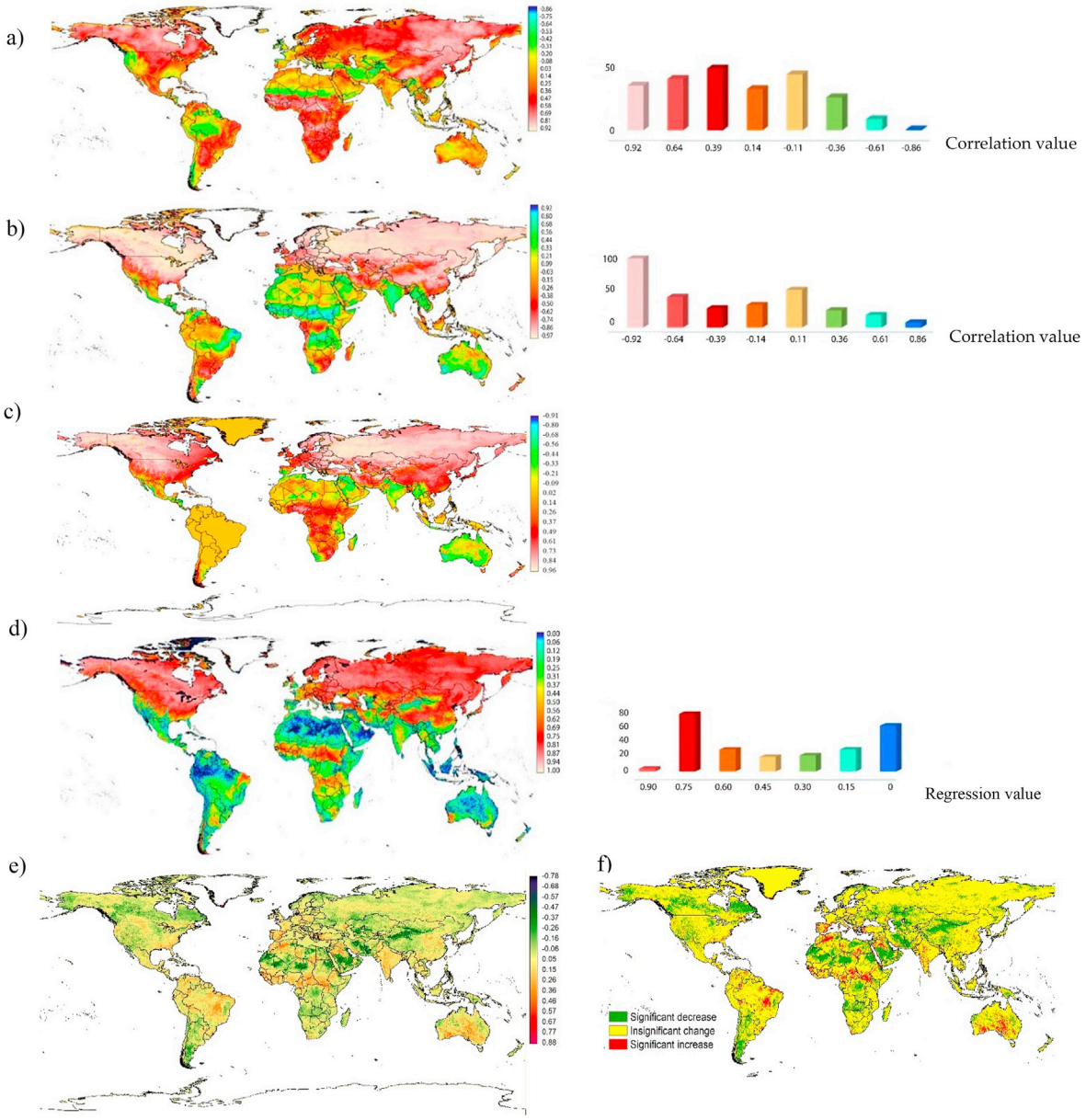

Fig. 9. Frequency graph of distribution, and each correlation model of dependent variable is vegetation and independent variable is climatic factors with or without time lag. (a) vegetation greenness and precipitation; (b) vegetation greenness and temperature; (c) vegetation greenness and solar radiation (d) spatial distribution map of the multiple linear regression model of vegetation greenness and climatic factors considering time-lag effects between 1982 and 2014, (e) trend residual of vegetation greenness, f) trend residual of types from 1982 to 2014.

impact in the Northern Hemisphere, precipitation has a higher global impact in all cropland areas (Fig. 9(b)). The areas with significant negative correlations include Australia, the Sahel, part of southern and northern Africa, central South America, and some regions of south Asia. Fig. 9(c) indicates that both precipitation and temperature greatly impact the vegetation in the Northern Hemisphere.

Our analysis also shows a strong and positive correlation (r = 0.89) between vegetation greenness and solar radiation over a 33-year period in the northern hemisphere (Fig. 9c). However, a negative correlation was detected (r = -0.47) for Australia, southern Asia and northern Africa.

The linear regression analysis based on the vegetation greenness residuals (Fig. 9d) showed a slightly increasing trend in the vegetation greenness residuals in India, central Africa, and Europe with positive rates. The vegetation greening up in these areas has largely exceeded the climate-only explanation, suggesting that improvements in vegetation conditions may be due to afforestation and ecological projects as well as population migration (positive impact) or increased cropland. A slight decreasing trend in the vegetation greenness residuals in the southwest Asia, central Asia, and north Africa is evident. Here, vegetation growth was lower than climate change expectations, indicating that human activity may lead to vegetation degradation (negative impact). The proportion of the area of significant decrease in vegetation greenness of residuals is approximately 30.5%, and insignificant change in vegetation greenness of residuals is 52.2%. The areas with significant increasing trends in the vegetation of the residuals accounted for 15.3%.

Our study detected a higher correlation (r = 0.88) between vegetation greenness and precipitation in the forest cover of Russia, Canada, northeast Asia, and central Africa. The results from our study (Fig. 10(a)) are in agreement with previous research by Seftigen et al. (2018), with vegetation greenness and temperature in the forest cover in the northern latitudes, and the highest negative correlation value (r = −0.60) was confined to most of Canada, North America, Europe, northeast Asia, and east China, whereas the Southern Hemisphere forest cover exhibited positive correlation, and in small areas, there was a lower correlation. There were medium correlations between vegetation greenness and precipitation in the forest cover of Europe; however, there was no correlation between vegetation greenness and precipitation in the forest cover of the Amazon, as was previously mentioned (Zhao et al., 2017), for western and southeastern North America, southeastern Asia, and western Europe. We found that between 1982 and 2014, the vegetation greenness trend decreased overall, with the largest declines detected in Argentina, western South America, North America, Canada, Central Africa, northern Africa, Saudi Arabia, south Asia, and northeast Asia. These findings were also confirmed by Piao et al. (2014). To discover how the ongoing climate factors,

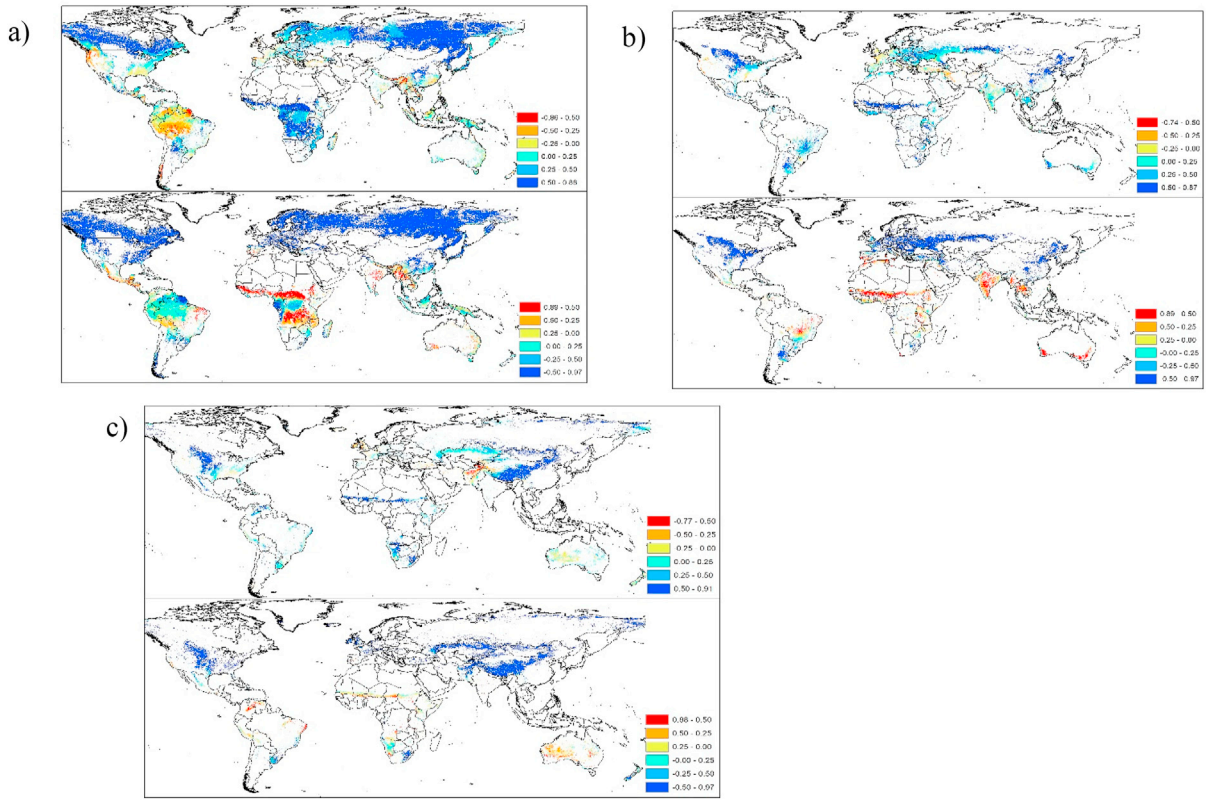

Fig. 10. Correlations of vegetation greenness and climate factors between 1982 and 2014 extracted by primary land cover. (a) Forest area: (top) vegetation greenness and rainfall; (bottom) vegetation greenness and temperature.(b) Cropland: (top) vegetation greenness and rainfall; (bottom) vegetation greenness and temperature. (c) Grassland: (top) vegetation greenness and rainfall; (bottom) vegetation greenness and temperature.

affect primary land cover (forest, cropland, and grassland), we analyzed the correlations between the vegetation greenness and climate factors (precipitation, temperature) on the forest cover in Fig. 10(a). The correlation results for grassland were tested statistically and are shown in Fig. 10(c). It was found that the vegetation greenness is highly correlated with rainfall in central Asia, North America, and Africa for grassland; however, some of the grassland regions of Australia and south Asia exhibited no correlation. The correlation distribution of the estimated values of vegetation greenness and temperature occurring within the grassland area is given in the bottom part of Fig. 10(c). In most of the Northern Hemisphere, there is a high negative correlation; however, in the Southern Hemisphere, we found a positive correlation in the grassland area.

4. Discussion

Our findings signal caution in the last 33 years, in which vegetation greenness exhibits a downward trend in the four seasons in the mid-latitude regions and in the southern part of the world. Similar findings were also reported by Hansen et al. (2013). A study by de Jong et al. (2011) have also reported that greening was mainly found in areas with relatively sparse vegetation cover in the Australian rangelands, African open shrubland, and the Sahel, mostly in combination with gradual browning, whereas abrupt browning was detected in more densely vegetated regions of the broadleaf forest in Europe and North America, and in the humid grasslands. Increasing temperature and decreasing precipitation are significantly correlated with decreasing vegetation greenness in our study. Specifically, temperature and vegetation greenness are indirectly correlated while precipitation is directly positively correlated. Under the current global warming scenario, both temperature increase and precipitation decrease are caused by global climate change (Zhao et al., 2018; Wang et al., 2011). Similar findings were also published by other researchers (Zhao et al., 2018; Wang et al., 2011; Lamchin et al., 2016), who confirmed that greening appears to have stopped and browning may have become predominant in the last decade in the Northern Hemisphere. However, the same studies reported more permanent browning periods in the Southern Hemisphere, especially in some parts of Argentina and Australia (De Jong et al., 2012). Some researchers reported that, three major driving factors affecting vegetation growth are climatic factors (Peteet, 2000; Nemani et al., 2003; Pearson et al., 2013; Peng et al., 2013), human activity, and natural disturbances (Bala et al., 2007; Malhi et al., 2008; Choat et al., 2012; Sterling et al., 2013; Brando et al., 2014; Zhang and Liang, 2014). A study by Wu et al. (2015), confirmed that human activity and natural disturbances are the key drivers of variations of vegetation growth. Human activity can positively or negatively impact vegetation greenness. For example, a study by Hicke et al. (2002) found that vegetation greenness has significantly increased over the past 27 years in eastern and southern America, owing to forest management interventions. The study also confirmed that there was no change in the climatic factors during the study period. On the contrary, cropland abandonment related to human activity, population growth, and livestock grazing is proven to negatively impact the NDVI (Jiang et al., 2017a,b; Erb et al., 2017).

An interesting finding is that the vegetation greenness of three cycles calculated over 10 years across global tropical drylands in the Amazon, Sahel, and in western Australia, indicated an upward trend from 1992 to 2002 (Fig. 2). However, a reverse trend was detected for the next ten years (2002–2014) in the same area. Factors such as lack of rainfall and drought could have contributed to this decreasing trend between 2002 and 2014. Our study indicated an increasing trend in precipitation in the first 10 years of our study, which could have led to increasing vegetation greenness. However, precipitation decreased during the second decade of our study, causing drought, which is related to decreasing vegetation greenness during that period. In fact, a drought was reported in the tropical drylands in 2010 (Xu et al., 2011). Such an incidence of drought can generate browning effects, causing vegetation greenness to drop. Although the discourse on whether greenness declined in the early part of the 21st century is not well settled (Medlyn, 2011; Samanta et al., 2011; Zhang et al., 2017; Zhao and Running 2010, 2011·bib_Zhao_and_Running_2010·bib_Zhao_and_Running_2011; Pan et al., 2018), scientists have converged to the fact that vegetation is decreasing at the regional scale. Other anthropogenic factors, including cropland expansion (Lamchin et al., 2016) and fallow land (Seftigen et al., 2018; Jiang et al., 2017a,b), have exacerbated the decreasing vegetation trends.

We observed that in the first ten-year period, precipitation trends upwards or downwards. In the next ten-year period, the trends are reversed, and in the final ten-year period showed trends that similar to the first ten-year period. For example, in the southeastern part of Australia, precipitation shows an upward (0.18) trend from 1982 to 1992 but a downward trend (−0.15) from 1993 to 2003 and an upward (0.14) again from 2004 to 2014 (Fig. 3). The study confirmed that the precipitation declined in all four seasons in southern South America and showed the same downward trend in the March–May and June–August periods from 1982 to 2014 in Australia. This demonstrates decreased precipitation in the southern part of the globe over the last 33 years. We also found that the trend of precipitation decreased the most in the March–May season in the majority of the areas. This season is also the most important time (onset) for vegetation growth in the Northern Hemisphere. A study by Angert et al. (2005) asserted that the earlier onset of greening in spring might be counter-balanced by lower productivity in the late summer. However, our study shows a greening trend in central South America, southern Africa, western Europe, and some parts of Australia. Moreover, during this time, in eastern China, western Kazakhstan, and western North America, increases in both greening and temperature were exhibited.

June–August is the growing and summer season in the mid-latitude regions of the Northern Hemisphere; however, as noted above in our study, rainfall decreased in all four seasons in many regions, whereas in the December–February and March–May seasons, increased temperature may influence ongoing drought and is related to the resulting vegetation greenness, with a downward trend in all four seasons in the mid-latitude region and Southern Hemisphere.

The temperature was found to be an important factor in influencing the forest areas in northern part and decreasing the forest cover; however, the temperature showed a lower correlation and was not the most important factor in the southern part of the globe in the Amazon and tropical zone. Similar findings were reported by other studies (Seftigen et al., 2018; Wu et al., 2017; Yang et al., 2018). Globally, for the recent 12-year period, gross forest cover losses accounted for 60.7 Mha (Hansen et al., 2013). Forest cover plays an important role in sequestering CO_2 and regulating water resources (Frank et al., 2015). The significant, highest positive correlations mainly appear in the Northern Hemisphere, suggesting that temperature is the most important factor that controls vegetation growth. Similarly, radiation, precipitation, and temperature were reported as major factors for rainforest, arid and semi-arid areas, and northern latitudes, respectively (Nemani et al., 2003; Wu et al., 2015; Lamchin et al., 2018). Our study confirmed that solar radiation was significantly correlated with vegetation greenness.

We confirm that a decreasing vegetation greenness for grassland cover during the last 33 years in central, south, and northeast Asia, Australia, and Africa. A loss of global grasslands by over 40% since the industrial era has led to a decline in ecosystem services (Veldman et al., 2015; White et al., 2000).

Our result finds decreasing precipitation trends in the desert of some part in north Africa, north part of Arabia and rainforest areas; however, in the greenness did not decrease. This can be attributed to desert plants that have better adaptive capacities, particularly to drought (Lamchin et al. 2015, 2018·bib_Lamchin_et_al_2018·bib_Lamchin_et_al_2015).

5. Conclusions

Climatic factors, especially temperature, precipitation, and solar radiation are known to affect vegetation greenness by reducing or increasing vegetation growth. This relationship has increasingly become complex with unpredictable impacts of climate change, making it difficult to ascertain global trends. This study used remotely sensed, climate and land cover data over 33 years to determine the relationship between vegetation greenness and climate variables by season, over 10-year intervals. Key conclusions from the study are enumerated below:

- Overall, our results indicate that vegetation greenness decreased over the study period, especially in the Northern Hemisphere. Our study also found that this period was associated with an increasing trend for temperature and a decreasing trend for precipitation, largely in the Northern Hemisphere. This leads us to conclude that this decrease is directly correlated with precipitation and indirectly correlated with temperature.
- Further, we conclude that this decreasing trend is more prominent during the spring seasons (March–May), especially in the Northern Hemisphere. This is an interesting finding, as spring should be the start of the growing season and it is expected to be associated with increasing vegetation greenness. This anomaly is probably a confirmation that spring is arriving later in most areas of the world. However, the trend reverses for the period of June to August, especially in the Northern Hemisphere, and this could be attributed to the impact of increasing precipitation. This finding is confirmed by the negative correlation between vegetation greenness and temperature ($r = -0.92$) in most parts of the Northern Hemisphere, whereas, a positive correlation ($r = 0.39$) was found in the southern hemisphere for cropland.
- The result suggests decreasing vegetation of greenness in 26.8% of the total forest cover in the cold zone. Furthermore, increasing vegetation of greenness was observed in 31.4%, whereas a decreasing trend was observed in 23.5% of the forest cover in the tropical zone.
- Further analysis by main land cover types showed a significant decrease in forest cover ($P < 0.05$) associated with increasing cropland. Increasing cropland has the potential to reduce vegetation greenness by 9.7% and, together with decreasing forest cover, was partly responsible for causing the vegetation greenness to decline.

In summary, we conclude that increasing temperature triggers drought conditions and amplifies desertification, especially in the semi-arid areas of the globe. This, topped with decreasing forest cover and increasing cropland, has primarily resulted in a global decrease in vegetation greenness. In addition, the strange variabilities of relationships between vegetation greenness in our study lead us to infer that climate change impacts are becoming unpredictable, highlighting the importance of trend monitoring analysis. Given this, we recommend further research to identify best practices to counter the loss of vegetation, desertification, and alleviate climate change impacts without hurting the livelihoods of the local people in the mid-latitude region.

Funding

This work was supported by the National Research Foundation of Korea grant of the Ministry of Education (No. 2018R1D1A1B07050437), and Ministry of Science and ICT (No. No. 2018R1A2B6005682), and Korea University grant.

Declaration of competing interest

The authors declare that they have no known competing financial interests or personal relationships that could have appeared to influence the work reported in this paper.

Acknowledgments

We thank three anonymous reviewers and editors for their valuable comments and suggestions.

References

Angert, A., Biraud, S., Bonfils, C., 2005. Drier summers cancel out the CO_2 uptake enhancement induced by warmer springs. Proc. Nat. Acad. Sci. USA 102, 10823–10827.
Anyamba, A., Tucker, C.J., 2005. Analysis of Sahelian vegetation dynamics using NOAA-AVHRR NDVI data from 1981–2003. J. Arid Environ. 63, 596–614.
Bala, G., Caldeira, K., Wickett, M., Phillips, T.J., Lobell, D.B., Delire, C., Mirin, A., 2007. Combined climate and carbon-cycle effects of large-scale deforestation. Proc. Natl. Acad. Sci. Unit. States Am. 104, 6550–6555.
Brando, P.M., Balch, J.K., Nepstad, D.C., Morton, D.C., Putz, F.E., Coe, M.T., Silvério, D., Macedo, M.N., Davidson, E.A., Nóbrega, C.C., Alencar, A., Soares-Filho, B.S. , 2014. Abrupt increases in Amazonian tree mortality due to drought–fire interactions. Proc. Natl. Acad. Sci. Unit. States Am. 111, 6347–6352.
Buermann, W., Wang, Y., Dong, J., Zhou, L., Zeng, X., Dickinson, R.E., Potter, C.S., Myneni, R.B., 2002. Analysis of a multiyear global vegetation leaf area index data set. J. Geophys. Res. 107 (D22), 4646.
Chen, C., He, B., Yuan, W., Guo, L., Zhang, Y., 2019. Increasing interannual variability of global vegetation greenness. Environ. Res. Lett. 14 (12), 124005.
Choat, B., Jansen, S., Brodribb, T.J., Cochard, H., Delzon, S., Bhaskar, R., Bucci, S.J., Field, T.S., Gleason, S.M., Hacke, U.G., Jacobsen, A.L., Lens, F., Maherali, H., Martínez-Vilalta, J., Mayr, S., Mencuccini, M., Mitchell, P.J., Nardini, A., Pittermann, J., Pratt, R.B., Sperry, J.S., Westoby, M., Wright, I.J., Zanne, A.E., 2012. Global convergence in the vulnerability of forests to drought. Nature 491, 752–755.
Churkina, G., Running, S.W., 1998. Contrasting climatic controls on the estimated productivity of global terrestrial biomes. Ecosystems 1, 206–215.
Cleland, E.E., Chuine, I., Menzel, A., Mooney, H.A., Schwartz, M.D., 2007. Shifting plant phenology in response to global change. Trends Ecol. Evol. 22, 357–365.
Cohen, J., 1988. Statistical Power Analysis for the Behavioral Sciences, second ed. Hillsdale, New Jersey.
de Jong, R., de Bruin, S., de Wit, A., Schaepman, M.E., Dent, D.L., 2011. Analysis of monotonic greening and browning trends from global NDVI time-series. Remote Sens. Environ. 115, 692–702.
De Jong, R., Verbesselt, J., Schaepman, M.E., de Bruin, S., 2012. Trend changes in global greening and browning: contribution of short-term trends to longer-term change. Global Change Biol. 18, 642–655.
Eastman, J.R., Sangermano, F., Ghimire, B., Zhu, H., Chen, H., Neeti, N., Crema, S.C., 2009. Seasonal trend analysis of image time series. Int. J. Rem. Sens. 30, 2721–2726.
Eklundh, L., Olsson, L., 2003. Vegetation index trends for the african Sahel 1982–1999. Geophys. Res. Lett. 30.
Erb, K.H., Luyssaert, S., Meyfroidt, P., Pongratz, J., Don, A., Kloster, S., Kuemmerle, T., Fetzel, T., Fuchs, R., Herold, M., Haberl, H., Jones, C.D., Marín-Spiotta, E., McCallum, I., Robertson, E., Seufert, V., Fritz, S., Valade, A., Wiltshire, A., Dolman, A.J., 2017. Land management: data availability and process understanding for global change studies. Global Change Biol. 23, 512–533.
Evans, J., Geerken, R., 2004. Discrimination between climate and human-induced dryland degradation. J. Arid Environ. 57, 535–554.
Feng, M., Sexton, J.O., Channan, S., Townshend, J.R., 2015. A global, high-resolution (30-m) inland water body dataset for 2000: first results of a topographic–spectral classification algorithm. Int. J. Digit. Earth 1–21.
Fensholt, R., Rasmussen, K., 2011. Analysis of trends in the Sahelian 'rain-use efficiency' using GIMMS NDVI, RFE and GPCP rainfall data. Remote Sens. Environ. 115, 438–451.
Fensholt, R., Rasmussen, K., Nielsen, T.T., Mbow, C., 2009. Evaluation of Earth observation based long term vegetation trends — intercomparing NDVI time series trend analysis consistency of Sahel from AVHRR GIMMS, Terra MODIS and SPOT VGT data. Remote Sens. Environ. 113, 1886–1898.
Fensholt, R., Langanke, T., Rasmussen, K., Reenbreg, A., Prince, S.D., Tucker, C., Scholes, R.J., Le, Q.B., Bondeau, A., Eastman, R., Epstein, H., Gaughan, A.E., Hellden, U., Mbow, C., Olsson, L., Paruelo, J., Schweitzer, C., Seaquist, J., Wessels, K., 2012. Greenness in semi-arid areas across the globe 1981–2007—an Earth-observing satellite-based analysis of trends and drivers. Remote Sens. Environ. 121, 144–158.
Fensholt, Rasmus, Tobias, Langanke, Rasmussen, Kjeld, Reenberg, Anette, Prince, Stephen D., Tucker, Compton, Robert, J., Scholes, et al., 2012. Greenness in semi-arid areas across the globe 1981–2007—an Earth Observing Satellite based analysis of trends and drivers. Remote Sens. Environ. 121, 144–158.
Frank, D., Reichstein, M., Bahn, M., Thonicke, K., Frank, D., Mahecha, M.D., Smith, P., Velde, M., Vicca, S., Babst, F., Beer, C., 2015. Effects of climate extremes on the terrestrial carbon cycle: concepts, processes and potential future impacts. Global Change Biol. 21, 2861–2880.
Fu, Y.H., Zhao, H., Piao, S., Peaucelle, M., Peng, S., Zhou, G., Ciais, P., Huang, M., Menzel, A., Peñuelas, J., Song, Y., Vitasse, Y., Zeng, Z., Janssens, I.A., 2015. Declining global warming effects on the phenology of spring leaf unfolding. Nature 526, 104.
Guay, K.C., Beck, P.S.A., Berner, L.T., Goetz, S.J., Baccini, A., Buermann, W., 2014. Vegetation productivity patterns at high northern latitudes: a multi-sensor satellite data assessment. Global Change Biol. 20, 3147–3158.
Guo, M., Jing, L.I., Hongshi, H.E., Jiawei, X.U., Yinghua, J., 2018. Detecting global vegetation changes using Mann–Kendall (MK) trend test for 1982–2015 time period. Chin. Geogr. Sci. 28, 907–919.
Hansen, M.C., Potapov, P.V., Moore, R., Hancher, M., Turubanova, S.A., Tyukavina, A., Thau, D., Stehman, S.V., Goetz, S.J., Loveland, T.R., Kommareddy, A., Egorov, A., Chini, L., Justice, C.O., Townshend, J.R.G., 2013. High-resolution global maps of 21st-century forest cover change. Science 342, 850–853.
Harris, I., Jones, P.D., Osborn, T.J., Lister, D.H., 2014. Updated high-resolution grids of monthly climatic observations – the CRU TS3.10 dataset. Int. J. Climatol. 34, 623–642.
Helldén, U., Tottrup, C., 2008. Regional desertification: a global synthesis. Global Planet. Change 64, 169–176.
Heumann, B.W., Seaquist, J.W., Eklundh, L., Jönsson, P., 2007. AVHRR derived phenological change in the Sahel and Soudan, Africa, 1982–2005. Remote Sens. Environ. 108, 385–392.
Hicke, J.A., Asner, G.P., Randerson, J.T., Tucker, C., Los, S., Birdsey, R., Jenkins, J.C., Field, C., 2002. Trends in North American net primary productivity derived from satellite observations, 1982–1998. Global Biogeochem. Cycles 16 (2–1), 2–14.
Hirsch, R.M., Slack, J.R., Smith, R.A., 1982. Techniques of trend analysis for monthly water quality data. Water Resour. Res. 18, 107–121.
Huang, K., Xia, J., Wang, Y., Ahlström, A., Chen, J., Cook, R.B., Cui, E., Fang, Y., Fisher, J.B., Huntzinger, D.N., Li, Z., Michalak, A.M., Qiao, Y., Schaefer, K., Schwalm, C.H., Wang, J., Wei, Y.X., Xu, X., Yan, L., Bian, C.H., Luo, Y., 2018. Enhanced peak growth of global vegetation and its key mechanisms. Nat. Ecol. Evol. 2, 1897–1905.
Jeyaseelan, A.T., Roy, P.S., Young, S.S., 2007. Persistent changes in NDVI between 1982 and 2003 over India using AVHRR GIMMS (global inventory modeling and mapping studies) data. Int. J. Rem. Sens. 28, 4927–4946.
Jiang, L., Bao, A., Guo, H., Ndayisaba, F., 2017a. Vegetation dynamics and responses to climate change and human activities in Central Asia. Sci. Total Environ. 599, 967–980.
Jiang, M., Tian, S., Zheng, Z., Zhan, Q., He, Y., 2017b. Human activity influences on vegetation cover changes in Beijing, China, from 2000 to 2015. Rem. Sens. 9, 271.
Jin, G., Chen, K., Wang, P., Guo, B., Dong, Y., Yang, J., 2019. Trade-offs in land-use competition and sustainable land development in the North China Plain. Technol. Forecast. Soc. Change 141, 36–46.
Kosaka, Y., Xie, S., 2013. Recent global-warming hiatus tied to equatorial Pacific surface cooling. Nature 501, 403–407.
Kvamme, K., 2018. Getting around the black box: teaching (geophysical) data processing through GIS. J. Comput. Anal. Appl. 1, 74–87.
Lamchin, M., Park, T., Lee, J.Y., Lee, W.K., 2015. Monitoring of vegetation dynamics in the Mongolia using MODIS NDVIs and their relationship to rainfall by natural zone. J. Indian Soc. Remote Sens. 43, 325–337.

Lamchin, M., Lee, J.Y., Lee, W.K., Lee, E.J., Kim, M., Lim, C.H., Choi, H.A., Kim, S.R., 2016. Assessment of land cover change and desertification using remote sensing technology in a local region of Mongolia. Adv. Space Res. 57, 64–77.
Lamchin, M., Lee, W.K., Jeon, S.W., Wang, S.W., Lim, C.H., Song, C., Sung, M., 2018. Long-term trend and correlation between vegetation greenness and climate variables in Asia based on satellite data. Sci. Total Environ. 618, 1089–1095.
Luo, P., Kang, S., Apip, Z.M., Lyu, J., Aisyah, S., Binaya, M., Regmi, R.K., Nover, D., 2019. Water quality trend assessment in Jakarta: a rapidly growing Asian megacity. PLoS One 14, e0219009. https://doi.org/10.1371/journal.pone.0219009.
Lyu, J., Luo, P., Mo, S., Zhou, M., Shen, B., Nover, D., 2019. A quantitative assessment of hydrological responses to climate change and human activities at spatiotemporal within a typical catchment on the Loess Plateau. China. https://doi.org/10.1016/j.quaint.2019.03.027. (Accessed 30 March 2019). available online.
Luo, M., Sa, C., Meng, F., Duan, Y., Liu, T., 2020. Assessing extreme climatic changes on a monthly scale and their implications for vegetation in Central Asia. J. Clean. Prod. 122396.
Malhi, Y., Roberts, J.T., Betts, R.A., Killeen, T.J., Li, W., Nobre, C.A., 2008. Climate change, deforestation, and the fate of the Amazon. Science 319, 169–172.
Medlyn, B.E., 2011. Comment on "drought-induced reduction in global terrestrial net primary production from 2000 through 2009. Science 333, 1093.
Myneni, R.B., Keeling, C.D., Tucker, C.J., Asrar, G., Nemani, R.R., 1997. Increased plant growth in the northern high latitudes from 1981 to 1991. Nature 386, 698–702.
Myneni, R.B., Tucker, C.J., Asrar, G., Keeling, C.D., 1998. Interannual variations in satellite-sensed vegetation index data from 1981 to 1991. J. Geophys. Res. Atmos. 103, 6145–6160.
Nemani, R.R., Keeling, C.D., Hashimoto, H., Jolly, W.M., Piper, S.C., Tucker, C.J., Myneni, R.B., Running, S.W., 2003. Climate-driven increases in global terrestrial net primary production from 1982 to 1999. Science 300, 1560–1563.
Neeti, N., Eastman, J.R., 2011. A contextual Mann–Kendall approach for the assessment of trend significance in image time series. Trans. GIS 15, 599–611.
Olsson, L., Eklundh, L., Ardö, J., 2005. A recent greening of the Sahel—trends, patterns and potential causes. J. Arid Environ. 63, 556–566.
Pan, N., Feng, X., Fu, B., Wang, S., Ji, F., Pan, S., 2018. Increasing global vegetation browning hidden in overall vegetation greening: insights from time-varying trends. Remote Sens. Environ. 214, 59–72.
Pearson, R.G., Phillips, S.J., Loranty, M.M., Beck, P.S.A., Damoulas, T., Knight, S.J., Goetz, S.J., 2013. Shifts in Arctic vegetation and associated feedbacks under climate change. Nat. Clim. Change 3, 673–677.
Peng, S., Piao, S., Ciais, P., Myneni, R.B., Chen, A., Chevallier, F., Dolman, A.J., Janssens, I.A., Peñuelas, J., Zhang, G., Vicca, S., Wan, S., Wang, S., Zeng, H., 2013. Asymmetric effects of daytime and night-time warming on Northern Hemisphere vegetation. Nature 501, 88–92.
Peñuelas, J., Rutishauser, T., Filella, I., 2009. Phenology feedbacks on climate change. Science 324, 887–888.
Peteet, D., 2000. Sensitivity and rapidity of vegetational response to abrupt climate change. Proc. Natl. Acad. Sci. Unit. States Am. 97, 1359–1361.
Piao, S., Nan, H., Huntingford, C., Ciais, P., Friedlingstein, P., Sitch, S., Peng, S., Ahlström, A., Canadell, J.G., Cong, N., Levis, S., Levy, P.E., Liu, L., Lomas, M.R., Mao, J., Myneni, R.B., Peylin, P., Poulter, B., Shi, X., Yin, G., Viovy, N., Wang, T., Wang, X., Zaehle, S., Zeng, N., Zeng, Z., Chen, A., 2014. Evidence for a weakening relationship between interannual temperature variability and northern vegetation activity. Nat. Commun. 5, 5018. https://doi.org/10.1038/ncomms6018.
Purdy, A.J., Fisher, J.B., Goulden, M.L., Colliander, A., Halverson, G., Tu, K., Famiglietti, J.S., 2018. SMAP soil moisture improves global evapotranspiration. Rem. Sens. Environ. 219, 1–14.
Piao, S., Wang, X., Park, T., Chen, C., Lian, X., He, Y., et al., 2019. Characteristics, drivers and feedbacks of global greening. Nature Reviews Earth & Environment 1–14.
Samanta, A., Costa, M.H., Nunes, E.L., Vieira, S.A., Xu, L., Myneni, R.B., 2011. Comment on "Drought-induced reduction in global terrestrial net primary production from 2000 through 2009. Science 333, 1093.
Seftigen, K., Frank, D.C., Björklund, J., Babst, F., Poulter, B., 2018. The climatic drivers of normalized difference vegetation index and tree-ring-based estimates of forest productivity are spatially coherent but temporally decoupled in Northern Hemispheric forests. Global Ecol. Biogeogr. 27, 1352–1365.
Sen, P.K., 1968. Estimate of the regression coefficient based on Kendall's Tau. J. Am. Stat. Assoc. 63, 1379–1389.
Seneviratne, S.I., Donat, M.G., Mueller, B., Alexander, L.V., 2014. No pause in the increase of hot temperature extremes. Nat. Clim. Change 4, 161–163.
Slayback, D.A., Pinzon, J.E., Los, S.O., Tucker, C.J., 2003. Northern hemisphere photosynthetic trends 1982–99. Global Change Biol. 9, 1–15.
Sterling, S.M., Ducharne, A., Polcher, J., 2013. The impact of global land-cover change on the terrestrial water cycle. Nat. Clim. Change 3, 385–390.
Stockli, R., Vidale, P.L., 2004. European plant phenology and climate as seen in a 20-year AVHRR land-surface parameter dataset. Int. J. Rem. Sens. 25, 3303–3330.
Tabor, K., Williams, J.W., 2010. Globally downscaled climate projections for assessing the conservation impacts of climate change. Ecol. Appl. 20, 554–565.
Tian, F., Fensholt, R., Verbesselt, J., Grogan, K., Horion, S., Wang, Y., 2015. Evaluating temporal consistency of long-term global NDVI datasets for trend analysis. Remote Sens. Environ. 163, 326–340.
Trenberth, K.E., Dai, A., van der Schrier, G., Jones, P.D., Barichivich, J., Briffa, K.R., Sheffield, J., 2014. Global warming and changes in drought. Nat. Clim. Change 4, 17–22.
Tucker, C.J., Slayback, D.A., Pinzon, J.E., Los, S.O., Myneni, R.B., Taylor, M.G., 2001. Higher northern latitude normalized difference vegetation index and growing season trends from 1982 to 1999. Int. J. Biometeorol. 45, 184–190.
Tucker, C.J., Nicholson, S.E., 1999. Variations in the Size of the Sahara Desert from 1980 to 1997. Ambio, pp. 587–591.
Veldman, J.W., Buisson, E., Durigan, G., Fernandes, G.W., Le Stradic, S., Mahy, G., Negreiros, D., Overbeck, G.E., Veldman, R.G., Zaloumis, N.P., Putz, F.E., Bond, W.J., 2015. Toward an old-growth concept for grasslands, savannas, and woodlands. Front. Ecol. Environ. 13, 154–162.
Wang, X., Piao, S., Ciais, P., Li, J., Friedlingstein, P., Koven, C., Chen, A., 2011. Spring temperature change and its implication in the change of vegetation growth in North America from 1982 to 2006. Proc. Natl. Acad. Sci. Unit. States Am. 108, 1240–1245.
Wessels, K.J., van den Bergh, F., Scholes, R.J., 2012. Limits to detectability of land degradation by trend analysis of vegetation index data. Remote Sens. Environ. 125, 10–22.
White, R.P., Murray, S., Rohweder, M., Prince, S.D., Thompson, K.M.J., 2000. Grassland Ecosystems. World Resources Institute, Washington DC.
Whittaker, R.H., 1975. Communities and Ecosystems, second ed. Macmillan Publishing Co., Inc, New York.
Wolkovich, E.M., Cook, B.I., Allen, J.M., Crimmins, T.M., Betancourt, J.L., Travers, S.E., Pau, S., Regetz, J., Davies, T.J., Kraft, N.J.B., Ault, T.R., Bolmgren, K., Mazer, S.J., McCabe, G.J., McGill, B.J., Parmesan, C., Salamin, N., Schwartz, M.D., Cleland, E.E., 2012. Warming experiments underpredict plant phenological responses to climate change. Nature 485, 494–497.
Wu, D., Zhao, X., Liang, S., Zhou, T., Huang, K., Tang, B., Zhao, W., 2015. Time-lag effects of global vegetation responses to climate change. Global Change Biol. 21, 3520–3531.
Wu, J., Guan, K., Hayek, M., Restrepo-Coupe, N., Wiedemann, K.T., Xu, X., Wehr, R., Christoffersen, B.O., Miao, G., da Silva, R., de Araujo, A.C., Oliviera, R.C., Camargo, P.B., Monson, R.K., Huete, A.R., Saleska, S.R., 2017. Partitioning controls on Amazon forest photosynthesis between environmental and biotic factors at hourly to interannual timescales. Global Change Biol. 23, 1240–1257.
Xu, L., Samanta, A., Costa, M.H., Ganguly, S., Nemani, R.R., Myneni, R.B., 2011. Widespread decline in greenness of Amazonian vegetation due to the 2010 drought. Geophys. Res. Lett. 38, L07402. https://doi.org/10.1029/2011GL046824.
Xu, L., Myneni, R.B., Chapin, F.S., Callaghan, T.V., Pinzon, J.E., Tucker, C.J., Zhu, Z., Bi, J., Ciais, P., Tømmervik, H., Euskirchen, E.S., Forbes, B.C., Piao, S.L., Anderson, B.T., Ganguly, S., Nemani, R.R., Goetz, S.J., Beck, P.S.A., Bunn, A.G., Cao, C., Stroeve, J.C., 2013. Temperature and vegetation seasonality diminishment over northern lands. Nat. Clim. Change 3, 581–586.
Yang, J., Tian, H., Pan, S., Chen, G., Zhang, B., Dangal, S., 2018. Amazon drought and forest response: largely reduced forest photosynthesis but slightly increased canopy greenness during the extreme drought of 2015/2016. Global Change Biol. 24, 1919–1934.

Yao, Rui, Wang, Lunche, Huang, Xin, Chen, Xinxin, Liu, Zhengjia, 2019. Increased spatial heterogeneity in vegetation greenness due to vegetation greening in mainland China. Ecol. Indicat. 99, 240–250.
Yu, M., Wang, G., Chen, H., 2016. Quantifying the impacts of land surface schemes and dynamic vegetation on the model dependency of projected changes in surface energy and water budgets. J. Adv. Model. Earth Syst. 8, 370–386.
Zeng, G., Wang, Z., Wen, S., Jiang, J., Wang, L., Cheng, J., Tan, D., Xiao, F., Ma, S., Li, W., Luo, K., Naoumov, N.V., Hou, J., 2005. Geographic distribution, virologic and clinical characteristics of hepatitis B virus genotypes in China. J. Viral Hepat. 12, 609–617.
Zeng, H.Q., Jia, G.S., Epstein, H., 2011. Recent changes in phenology over the northern high latitudes detected from multi-satellite data. Environ. Res. Lett. 6, 1–11.
Zhang, Y., Liang, S., 2014. Changes in forest biomass and linkage to climate and forest disturbances over Northeastern China. Global Change Biol. 20, 2596–2606.
Zhang, Y., Song, C., Band, L.E., Sun, G., Li, J., 2017. Reanalysis of global terrestrial vegetation trends from MODIS products: browning or greening? Remote Sens. Environ. 191, 145–155.
Zhao, L., Dai, A., Dong, B., 2018. Changes in global vegetation activity and its driving factors during 1982–2013. Agric. For. Meteorol. 249, 198–209.
Zhao, M., Running, S.W., 2010. Drought-induced reduction in global terrestrial net primary production from 2000 through 2009. Science 329, 940–943.
Zhao, M., Running, S.W., 2011. Response to comments on “Drought-induced reduction in global terrestrial net primary production from 2000 through 2009. Science 333, 1093.
Zhao, W., Zhao, X., Zhou, T., Wu, D., Tang, B., Wei, H., 2017. Climatic factors driving vegetation declines in the 2005 and 2010 Amazon droughts. PLoS One 12, e0175379.
Zhou, L., 2001. Variations in northern vegetation activity inferred from satellite data of vegetation index during 1981 to 1999. J. Geophys. Res. 106, 20069–20083.